

Contents lists available at [SciVerse ScienceDirect](http://SciVerse.Sciencedirect.com)

# Journal of Computational and Applied Mathematics

journal homepage: [www.elsevier.com/locate/cam](http://www.elsevier.com/locate/cam)

## Innovative modelling of 3D unsaturated flow in porous media by coupling independent models for vertical and lateral flows

Raphaël Paulus\*, Benjamin J. Dewals, Sébastien Erpicum, Michel Piroton, Pierre Archambeau

University of Liège, Belgium

### ARTICLE INFO

#### Article history:

Received 31 January 2012

Received in revised form 24 July 2012

#### Keywords:

Richards equation

Groundwater modelling

Unsaturated Flow

Quasi three-dimensional

### ABSTRACT

Unsaturated groundwater flows are mathematically represented by the Richards equation. Hitherto, in Hydrology, solutions of this equation mainly serve as an alimentation of the source term for the surface runoff modelling. Therefore, the complete resolution of the 3D model looks surplus to requirements and the infiltration is dealt either thanks to 1D vertical modelling of the Richards equation or through derivate models (like e.g. the Green–Ampt infiltration model or the Horton law), thus ignoring eventual horizontal transfers.

Nowadays, the request for more detailed information is real, and the physics of groundwater unsaturated flow needs to be represented more reliably. This information could be furnished by the resolution of the complete 3D model, but, although numerically mastered and well documented, it is very costly for large scale – both in time and space – real applications (climate change adaptation of watersheds).

The authors propose an original solution decoupling the 3D equations into 1D vertical equations and a 2D depth-integrated horizontal equation. The aim is to consider independent vertical columns of infiltration coupled with lateral transfer of mass through the boundary conditions. On this basis, they postulate that the mass transfers in the three dimensions are correctly represented. This way problematic like the supply of the aquifers, the re-emergence of groundwater to surface water or especially the capability of memorization of past rainy events ... could be reliably depicted.

The two coupled models are solved on a unique numerical frame. A cell-centred Finite Volume method is used to solve the parabolic partial differential equations. The spatial derivatives are approximate by a second order central difference scheme, while the time splitting follows an implicit backward Euler scheme coupled with Picard iteration.

The method has been tested and its reliability assessed on different theoretical two-dimensional cross-sectional test cases representing infiltration phenomena.

© 2012 Elsevier B.V. All rights reserved.

### 1. Introduction

Within our laboratory of hydraulics in environmental and civil engineering, hydraulic unsteady phenomena have been studied for the past fifteen years, developing in this manner numerical and mathematical tools in order to simulate the widest possible range of mixed flows, from overland flow (using diffusive wave approximation models) to river networks (using 1D simulations) and more detailed local studies (using 2D and 2DV simulations). The whole numerical models compose the software package WOLF, which enables the simulation of hydrological runoffs (spatially distributed and

\* Correspondence to: Department ArGEnCO (Architecture, Geology, Environment and Constructions), HECE Unit (Hydraulics in Environmental and Civil Engineering), Ch. Des Chevreuils 1, B52/3+1, B-4000 Liege, Belgium. Tel.: +32 4 366 90 04; fax: +32 4 366 95 58.

E-mail address: [raphael.paulus@ulg.ac.be](mailto:raphael.paulus@ulg.ac.be) (R. Paulus).

process-oriented) [1]; 1D hydrodynamics, for both pressurized and free-surface flows [1–4] and 2D hydrodynamics, either as pure hydrodynamics, or coupled with air entrainment [4], sediment [5,6], or pollutant transport [7], or with turbulence models (including an original  $k-\varepsilon$  model [8]). Finally, an optimization tool, based on Genetic Algorithms [2] is available.

At the time when climate changes are at the centre of discussions, scientific topics like flood mitigations are in a state of ferment, and the multiple components of our modelling package are therefore in constant advancement, in order to meet the current needs, whether they are scientific or decision-making related [9,10]. It is in fact of great importance to furnish tools that enable to deal with recurrent environmental issues, and the request for more detailed and reliable solutions is as important as the need for fast and efficient representative models.

In this paper, the authors focus their researches on the groundwater modelling in the unsaturated zone. These transfers play a predominant role in the modelization of hydrological runoffs and, while common and simplistic assumptions like Green–Ampt models or Horton equations are sufficient to enable the calculation of flooding discharges [11,12], when it comes to a long period of time – thus including not only flood but also dry periods – more detailed representations of these process are required. Therefore, the recourse to the solving of the Richards equation is necessary.

The resolution of the complete 3D equations on large-scale basins leads to the consideration of very huge non-linear systems, whose numerical resolution is very costly. Besides, as our researches focus on the overland flow modelling, such an elaborate solution is out of the scope, with only the exchanges with the surface flow and the aquifers, as well as the horizontal transfers of water, to quantify in order to give a reliable representation of problems like the supply of the aquifers, the re-emergence of groundwater to surface water or especially the capability of memorization of past rainy events . . . Quasi three-dimensional models have been developed for the last fifty years, differing from the number of layers involved, from the nature of these layers (fully saturated flow or unsaturated flow) or from the equations used for the lateral transfers [13–16], with the major concern being a faithful representation of the water table and the 3-dimensional flow therein in order to meet environmental concerns – like e.g. the migration of solutes, that mainly occur in the saturated zone –, thus neglecting the possible lateral flows in the unsaturated zone, although at the same time, it has been pointed that these transfers can play a significant role [17]. The objective of this work is to compensate for this gap, which can be serious in the aforementioned circumstances. The key of the proposed model consists of the decomposition of the three-dimensional Richards Partial Differential Equation (PDE) into a one-dimensional vertical PDE and a two-dimensional depth-averaged PDE. This way, the number of unknowns that need to be solved in the non-linear systems is reduced dramatically, and a faster resolution is possible.

First, the solution method is introduced. Then, the different numerical models are presented and tested. Finally, the validity of the proposed model is assessed on two-dimensional cross-sectional test cases, and its efficiency is discussed.

## 2. Solution method

Since the critical point of the resolution consists of solving a system of the non-linear Richards equations, the fewer unknowns there are, the quicker the solution is obtained. Thus, it is decided to reduce the complete three-dimensional domain to multiple one-dimensional vertical columns (that can be solved independently one another) and one two-dimensional horizontal diffusion depth-integrated plan (Fig. 1). Moreover, as the vertical columns lead to reduced tri-diagonal systems, the computing time can be reduced further, by avoiding the need for iterative solvers.

By doing so, the author postulates that the mass fluxes are correctly represented.

Two modules are computed to solve each problem independently, both based on the same numerical scheme; a cell-centred Finite Volume scheme is used on structured Cartesian grids, and the non-linearity of the Richards equation is acquainted using Picard iteration. The interaction between these two models consists of a coupling between the two-dimensional horizontal layer and the boundary conditions of the one-dimensional vertical columns.

## 3. Mathematical and numerical model

The original method proposes to solve independently vertical and lateral transfers. These are depicted by the Richards equation whose resolution follows a specific numerical scheme.

In order to stay general, the formulation is global first; the flow equations, the soil properties equations, the numerical scheme and the boundary conditions are set out. Subsequently, the two specific modules are presented and discussed.

### 3.1. Set of equations

The Richards equation represents the water flow into a porous media. It consists of a combination of the mass balance and the momentum equations in porous media, i.e. the Darcy equation, giving the specific discharge.

$$\begin{cases} \frac{\partial \theta}{\partial t} + \nabla \vec{q} = S \\ \vec{q} = -k(\theta) \cdot \vec{\nabla} (z + \psi) \end{cases} \quad (1)$$

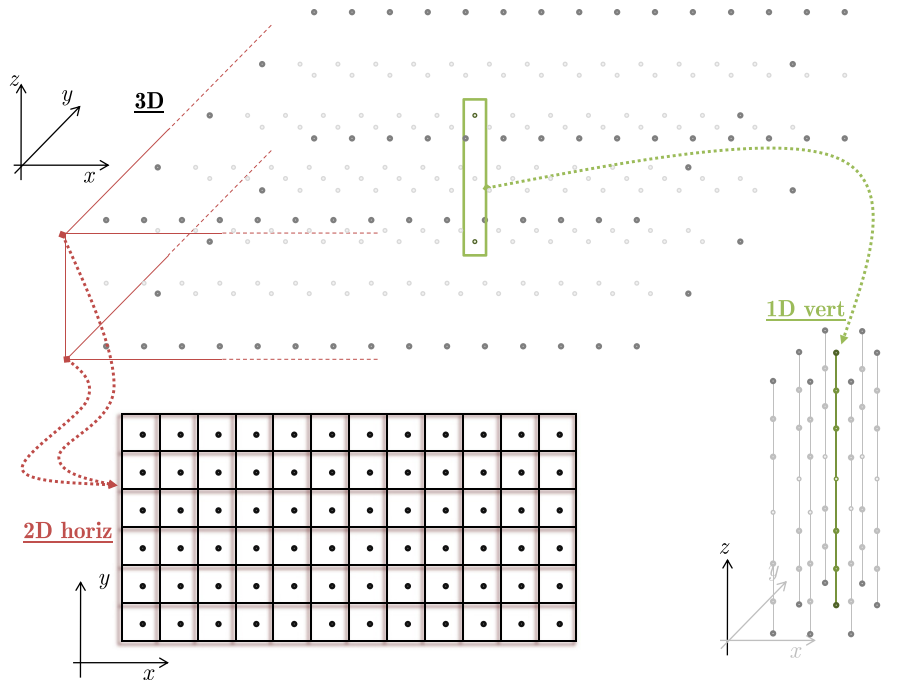


Fig. 1. Decomposition of the 3D layer into a 2D horizontal plan and multiple 1D-vertical columns.

$$\Rightarrow \frac{\partial \theta}{\partial t} + \nabla \left[ -k(\theta) \cdot \vec{\nabla} (z + \psi) \right] = S \tag{2}$$

$$\frac{\partial \theta}{\partial t} + \nabla \left[ -k(\theta) \cdot \vec{\nabla} (\psi) \right] - \frac{\partial k(\theta)}{\partial z} = S \tag{3}$$

with  $q$  (m/s) the specific discharge,  $\theta$  (–) the water content,  $k$  (m/s) the hydraulic conductivity,  $z$  (m) the vertical elevation (assumed positive upward),  $y$  (m) the pressure head and  $S$  ( $s^{-1}$ ) a possible source term.

### 3.2. Soils properties

The hydraulic conductivity can be determined by a soil–water model. In particular, one can mention the van Genuchten–Mualem (4)–(5) and Brooks–Corey (6)–(7) models [18,19], that are respectively presented hereafter.

$$\frac{\theta - \theta_r}{\theta_s - \theta_r} = \left[ \frac{1}{1 + (\alpha |\psi|)^n} \right]^{(n-1)/n} \tag{4}$$

$$\frac{K(\theta)}{K_s} = \left( \frac{\theta - \theta_r}{\theta_s - \theta_r} \right)^{1/2} \left\{ 1 - (\alpha |\psi|)^{n-1} \left[ 1 + (\alpha |\psi|)^n \right]^{(1-n)/n} \right\}^2 \tag{5}$$

$$\frac{\theta - \theta_r}{\theta_s - \theta_r} = \left[ \frac{\psi_b}{\psi} \right]^\lambda \tag{6}$$

$$\frac{K(\theta)}{K_s} = \left( \frac{\theta - \theta_r}{\theta_s - \theta_r} \right)^{3+2/\lambda} \tag{7}$$

with  $n$  (–),  $a$  ( $m^{-1}$ ),  $\psi_b$  (m) and  $\lambda$  (–) specific soil parameters,  $K_s$  (m/s) the hydraulic conductivity at saturation,  $\theta_s$  (–) the porosity and  $\theta_r$  (–) the residual water content.

Another suction curve frequently mentioned in experimental researches [20–22] lies as follow:

$$\frac{\theta - \theta_r}{\theta_s - \theta_r} = \frac{\alpha}{\alpha + |\psi|^\beta} \tag{8}$$

$$\frac{K(\theta)}{K_s} = \frac{A}{A + |\psi|^\gamma} \tag{9}$$

with  $A$  (–),  $\alpha$  ( $m^{-1}$ ),  $\gamma$  (–) and  $\beta$  (–) specific soil parameters.

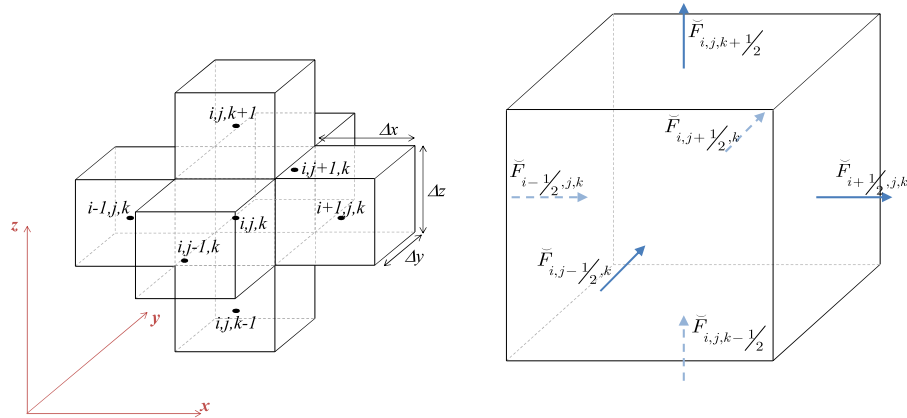


Fig. 2. –(left) regular grid –(right) fluxes through the edges of the meshes.

3.3. Numerical scheme of resolution for the Richards equation

A modified “head-based” formulation is used in order to guaranty mass conservation through the spatial discretization [23]. By use of the Green theorem, it leads to:

$$\iint_{\Omega} \frac{\partial \theta}{\partial t} d\Omega = \iint_{\Omega} \left( \frac{\partial}{\partial x} \left( k_x(\theta) \frac{\partial \psi}{\partial x} \right) + \frac{\partial}{\partial y} \left( k_y(\theta) \frac{\partial \psi}{\partial y} \right) + \frac{\partial}{\partial z} \left( k_z(\theta) \frac{\partial \psi}{\partial z} \right) + \frac{\partial k_z(\theta)}{\partial z} \right) d\Omega + \iint_{\Omega} S d\Omega \quad (10)$$

$$\frac{\partial}{\partial t} \iint_{\Omega} \theta d\Omega = \oint_{\Sigma} \left( k_x(\theta) \frac{\partial \psi}{\partial x} n_x + k_y(\theta) \frac{\partial \psi}{\partial y} n_y + k_z(\theta) \frac{\partial \psi}{\partial z} n_z + k_z(\theta) n_z \right) d\sigma + \iint_{\Omega} S d\Omega \quad (11)$$

$$|\Omega| \frac{\partial \theta}{\partial t} = \sum_{l=1}^{n_{edges}} \left( k_x(\theta) \frac{\partial \psi}{\partial x} n_x + k_y(\theta) \frac{\partial \psi}{\partial y} n_y + k_z(\theta) \frac{\partial \psi}{\partial z} n_z + k_z(\theta) n_z \right)_l |\Sigma_l| + |\Omega| |S|. \quad (12)$$

We consider a cell-centred finite volume method and a regular grid (Fig. 2(-left)).

Due to the parabolic form, the spatial discretization is performed using 2nd order central difference scheme for the spatial derivatives.

In terms of fluxes (Fig. 2-right), Eq. (12) is rewritten:

$$\Delta V \frac{\partial \theta_{i,j,k}}{\partial t} = \left\{ \left( \check{F}_{i+1/2,j,k} - \check{F}_{i-1/2,j,k} \right) \Delta y \Delta z + \left( \check{F}_{i,j+1/2,k} - \check{F}_{i,j-1/2,k} \right) \Delta x \Delta z + \left( \check{F}_{i,j,k+1/2} - \check{F}_{i,j,k-1/2} \right) \Delta x \Delta y \right\} + |\Omega_{i,j}| \Delta V \quad (13)$$

$$\begin{cases} \check{F}_{i\pm 1/2,j,k} = k_x(\theta) |_{i\pm 1/2,j,k} \frac{\partial \psi}{\partial x} \Big|_{i\pm 1/2,j,k} = k_x(\theta) |_{i\pm 1/2,j,k} \left( \frac{\mp \psi_{i,j,k} \pm \psi_{i\pm 1,j,k}}{\Delta x} \right) \\ \check{F}_{i,j\pm 1/2,k} = k_y(\theta) |_{i,j\pm 1/2,k} \frac{\partial \psi}{\partial y} \Big|_{i,j\pm 1/2,k} = k_y(\theta) |_{i,j\pm 1/2,k} \left( \frac{\mp \psi_{i,j,k} \pm \psi_{i,j\pm 1,k}}{\Delta y} \right) \\ \check{F}_{i,j,k\pm 1/2} = k_z(\theta) |_{i,j,k\pm 1/2} \frac{\partial \psi}{\partial z} \Big|_{i,j,k\pm 1/2} + k_z(\theta) |_{i,j,k\pm 1/2} = k_z(\theta) |_{i,j,k\pm 1/2} \left( \frac{\pm \psi_{i,j,k} \mp \psi_{i,j,k\pm 1}}{\Delta z} \right) \\ + k_z(\theta) |_{i,j,k\pm 1/2}. \end{cases} \quad (14)$$

As proposed by Celia et al. [23], the time splitting follows an implicit backward Euler scheme:

$$\frac{\theta^{t+1} - \theta^t}{\Delta t} - S = \nabla \left[ k(\theta) \cdot \vec{\nabla}(\psi) + \frac{\partial K}{\partial z} \right]^{t+1}. \quad (15)$$

The non-linearity of the conductivity coefficients is solved using Picard iteration [23], which is a very simple and intuitive method that is widely used for dealing with the non-linearity of the Richards equation; its forces being a low computational cost per-iteration and an easiness of implementation, while its major drawback lies in its slow convergence, yet it is completely appropriate in the frame of our developments, as indicated by Paniconi and Putti [24].

$$\frac{\theta^{t+1,m+1} - \theta^t}{\Delta t} - S = \nabla \left[ k(\theta^{t+1,m}) \cdot \vec{\nabla}(\psi^{t+1,m+1}) + \frac{\partial K(\theta^{t+1,m})}{\partial z} \right]. \quad (16)$$

And along with Taylor expansion of the water-content term (17) at the iterative level  $m$ , it leads to the final expression (18),

$$\begin{aligned} \theta^{t+1,m+1} &= \theta^t + \frac{\partial \theta}{\partial \psi} \Big|_{t+1,m} (\psi^{t+1,m+1} - \psi^{t+1,m}) \\ &= \theta^{t+1,m} + \eta^{t+1,m} (\psi^{t+1,m+1} - \psi^{t+1,m}) \end{aligned} \tag{17}$$

$$\Rightarrow \frac{\theta^{t+1,m} + \eta^{t+1,m} (\psi^{t+1,m+1} - \psi^{t+1,m}) - \theta^t}{\Delta t} - S = \nabla \left[ k(\theta^{t+1,m}) \cdot \vec{\nabla} (\psi^{t+1,m+1}) + \frac{\partial K(\theta^{t+1,m})}{\partial z} \right] \tag{18}$$

which is a linear system of equations. Its solution is obtained by an iterative method at each time step (the solver of the Generalized Minimal RESidual method [25] is used) with an arbitrary convergence criterion [26].

### 3.4. Boundary conditions

The boundary conditions can be of two mathematical types, depending on whether a pressure head (Dirichlet boundary condition) or a flux (von Neuman boundary condition) is imposed, and must be fixed on the whole boundary (parabolic PDE). A third type of boundary condition can be encountered in the presence of seepage face. The location of this face, and the subsequent imposition of the boundary value right there, is solved using Neuman’s iterative procedure [27,28].

In our model, the boundary conditions are forced on the edges of the meshes, and their impacts in terms of fluxes are evaluated thanks to Eqs. (14).

Several authors [29,30] discuss the adequate choice of exchange boundary conditions between the groundwater flow and the surface flow, which is considered independently [1,11,31,32]. In this paper, this interface is not taken into consideration, and the model is assessed only on its own.

### 3.5. Vertical transfer

The first component of the proposed integrated model consists of multiple vertical columns that transfer the fluxes along the  $z$ -axis. This model is obtained straight from the complete model, simply by ignoring the non-relevant terms. The equation for this model therefore stands as:

$$\frac{\partial \theta}{\partial t} + \frac{\partial}{\partial z} \left[ -k(\theta) \cdot \frac{\partial}{\partial z} (\psi) \right] - \frac{\partial K}{\partial z} = S \tag{19}$$

and the spatial discretization then leads to:

$$\begin{aligned} \frac{\partial \theta_{i,j}}{\partial t} &= \psi_{i,j} \left( \frac{-k_z(\theta) |_{i,j-1/2} - k_z(\theta) |_{i,j+1/2}}{\Delta z^2} \right) + \psi_{i,j-1} \left( \frac{k_z(\theta) |_{i,j-1/2}}{\Delta z^2} \right) + \psi_{i,j+1} \left( \frac{k_z(\theta) |_{i,j+1/2}}{\Delta z^2} \right) \\ &\quad + \frac{k_z(\theta) |_{i,j-1/2} - k_z(\theta) |_{i,j+1/2}}{\Delta z} + |\Omega_{i,j}| |S_{i,j}| \end{aligned} \tag{20}$$

with the time splitting giving the same scheme as (18).

Following recommendations of [30], a harmonic mean is used in order to estimate the hydraulic conductivity on the edges.

In Eq. (20), the values of only three cells are involved, and, by using an adequate numbering during the meshing, the system then becomes tri-diagonal. A direct resolution is therefore possible, and the Thomas Algorithm is used in this manner [33].

### 3.6. Lateral diffusion

The second component of the proposed integrated model consists of the horizontal diffusion of the fluxes through an integrated depth with the consideration of impervious boundaries. This depth-average of (3) leads to:

$$\frac{\partial}{\partial t} |\theta|_{depth} + \frac{\partial}{\partial x} \left[ -|k(\theta)|_{depth} \cdot \vec{\nabla} |\psi|_{depth} \right] + \frac{\partial}{\partial y} \left[ -|k(\theta)|_{depth} \cdot \vec{\nabla} |\psi|_{depth} \right] = 0 \tag{21}$$

This equation simply means the mass conservation for the depth-averaged unknowns (the symbols  $|\cdot|_{depth}$  representing the depth-average value of the unknown in brackets). Therefore, the spatial and time discretization are similar to the ones presented before ((18) and (20)).

Arithmetic means have been used for all the average unknowns ( $|\cdot|_{depth}$  terms); while the hydraulic conductivity on the edges is evaluated as for the one-dimensional vertical model, on the basis of the depth-averaged value.

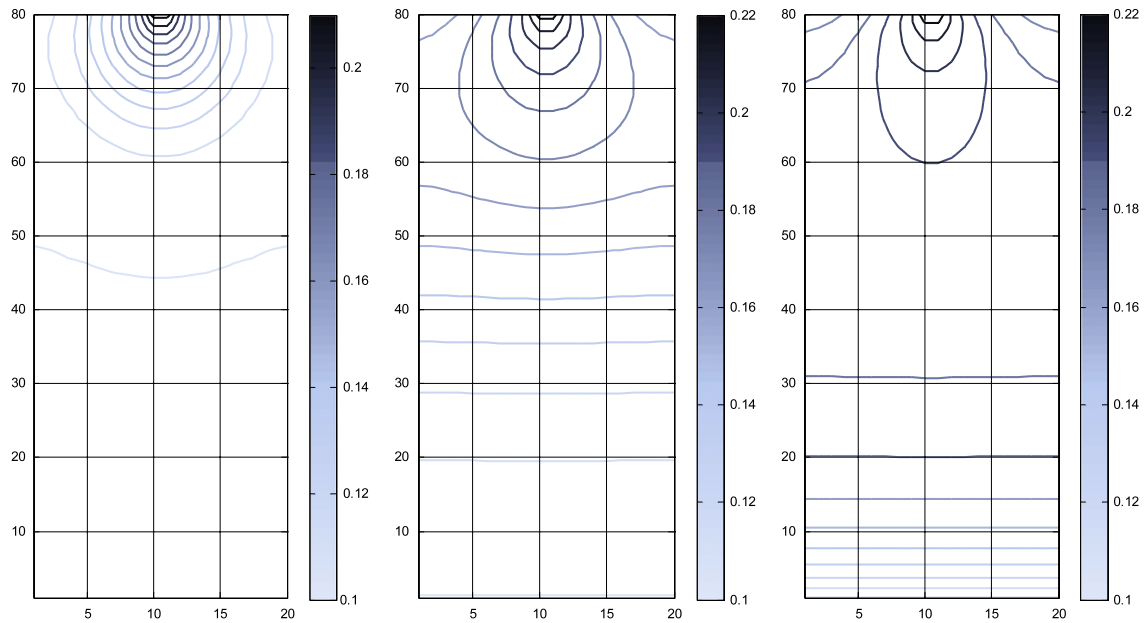


Fig. 3. The isovalues of water content (—) after 10 min, 1 and 4 h show agreement with an expected behaviour from a curvature point of view.

#### 4. Validation of the numerical model

In the literature, many validation examples can be found for one-dimensional infiltration cases [22,23,34–36], and some as well for two-dimensional vertical infiltration and drainage cases [21,37,38]. However, for the complete three-dimensional behaviour, most of the benchmarks available refer to the global hydrological behaviour – with the consideration of overland flow and evapotranspiration among others – and the validity is assessed by comparison with climatic data and *in situ* measurements [39]. As for now, the proposed method depicted in this paper is not implemented in our global hydrological model, and such simulation can therefore not be run. The validity of the proposed model will thus only be assessed on two-dimensional cross-sectional test cases.

First, the numerical scheme is assessed by the analysis of two-dimensional cross-sectional test cases. Then, the one-dimensional vertical model is as well validated. For the lateral diffusion, the validation on its own is not from great interest, given that the result only serves as an input for the vertical columns, through the monitoring of the boundary conditions.

Numerous test cases have been implemented, differing in the type of boundary conditions and in the nature of the process involved mainly. Here four test cases are outlined, with the objective to prove the validity and the robustness of the numerical scheme. In fact, the model deals as well under sharp saturation front than under free drying.

##### 4.1. Qualitative analysis of transient infiltration in a two-dimensional soil column

The qualitative comparison is based on experimental observations made in the middle of last century at the Washington State University [40], which depicts the infiltration into a homogeneous soil at a constant rate (Fig. 3).

The sample is a sandy-clay-loam soil box with impervious edges. The Brooks–Corey model is used to model the soil, with  $\theta_r = 0.068$  (–),  $\theta_s = 0.398$  (–),  $\psi_b = -0.5941$  (m),  $\lambda = 0.319$  (–) and  $K_s = 1.19 \cdot 10^{-6}$  (m/s). The infiltrated discharge corresponds to the hydraulic conductivity at saturation. The initial state is a constant pressure head of  $-0.5$  (m) over the whole domain. As for the numerical parameters,  $\Delta x = \Delta z = 0.01$  (m),  $\Delta t = 10$  (s). The simulation is performed during 12 (h).

##### 4.2. Two-dimensional transient flow in unsaturated–saturated soils

Two examples are depicted and discussed in this section. Both of them represent experiments that have been presented by Vauclin, concerning the recharge of a water table for the first one [21] and the drainage of a water table for the second one [20]. The flow domain consists of a rectangular box of 600 (cm) long and 200 (cm) high.

For the first test case, a water table is initially imposed at a depth of 135 (cm), and the initial state represents a hydrostatic equilibrium. At the soil surface, a constant flux of 14.8 (cm/h) is applied over a width of 100 (cm) in the centre. The bottom is impervious and a water level is maintained on both lateral sides of the box, at the depth of the initial water table. Due to

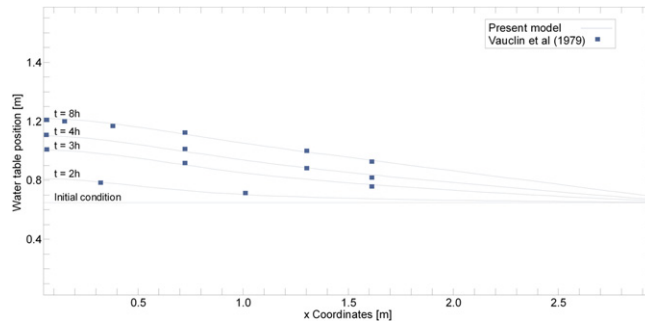


**Fig. 4.** The simulation of the water table position at different time of the experiment shows a good agreement with the experimental results.

the symmetry of the problem, the numerical simulation is performed on a  $300 \times 200$  (cm) box. The boundary conditions look the following way:

- on the left lateral side: no-flow (vonNeuman), by symmetry;
- at the bottom: no-flow (vonNeuman);
- at the top: flux on the first 50 (cm) and no-flow on the rest (vonNeuman);
- on the right lateral side: pressure or no-flow as a function of the external water table and the seepage face position.

The soil parameters, for the water-curve Eqs. (8)–(9), are  $\theta_r = 0.00$  (–),  $\theta_s = 0.30$  (–),  $\alpha = 40\,000$  (m),  $\beta = 2.90$  (–) and  $K_s = 35$  (cm/h),  $A = 2.99 \cdot 10^6$ ,  $B = 5.0$  (see Fig. 4).

For the second test case, a water table is initially imposed at a depth of 55 (cm), and the initial state represents a hydrostatic equilibrium. When the experiment begins, the water table is suddenly dropped 70 (cm) below the initial position. The bottom is impervious and a water level is maintained on both lateral sides of the box, at the depth of the initial water table. Due to the symmetry of the problem, the numerical simulation is performed on a  $300 \times 200$  (cm) box. The boundary conditions look the following way:

- on the left lateral side: no-flow (vonNeuman), by symmetry;
- at the bottom: no-flow (vonNeuman);
- at the top: no-flow (vonNeuman);
- on the right lateral side: pressure or no-flow as a function of the external water table and the seepage face.

The soil parameters, for the water-curve Eqs. (8)–(9), are now  $\theta_r = 0.00$  (–),  $\theta_s = 0.30$  (–),  $\alpha = 40\,000$  (m),  $\beta = 2.90$  (–) and  $K_s = 35$  (cm/h),  $A = 359\,720$ ,  $B = 4.0$  (see Fig. 5).

#### 4.3. Transient infiltration in a one-dimensional vertical soil column

As said before, the one-dimensional vertical infiltration model can be validated by comparison tests with different literature benchmarks [41]. Here we present a validation on a test case presented in [34,42], which consists of an infiltration (the boundaries consists of water-head (cm) imposition) in a New-Mexico soil modelled by a vanGenuchten–Mualem water-retention curve [43]; with  $\theta_r = 0.102$  (–),  $\theta_s = 0.368$  (–),  $\alpha = -0.0335$  ( $\text{cm}^{-1}$ ),  $n = 2$  (–) and  $K_s = 9.22 \cdot 10^{-3}$  (cm/s). The initial state is a constant pressure head of  $-1000$  (cm). As for the numerical parameters,  $\Delta z = 0.04$  (m),  $\Delta t = 120$  (s). The simulation is performed during 48 (h) (Fig. 6).

## 5. Integrated model

A global algorithm has been developed to ensure the propagation of the fluxes through the unsaturated soil. As introduced earlier, it consists of the coupling of a module for the vertical transfers and another one for the lateral diffusion.

The coupling between the two modules follows a specific 3-step scheme in order to progress from one time step (Fig. 7). At the time step  $t$ , the solution is known on the whole domain, in terms of pressure head and water content.

Without going into further details, one can mention that the boundary's behaviour can be obtained by a coupling with the other components of the hydrological runoff, so be it the overland flow and the atmospheric conditions at the top, and the fully-saturated flow at the bottom, thus it is forced and known before the beginning of the coupling process.

The three step procedure introduced in Fig. 7 splits the resolution in such a way that the solution at the next time step consists of the solution of the vertical columns (step 3) on the basis of boundary conditions that correspond to the depth-integrated lateral diffusion (step 2) of the discharges forced by the boundary's behaviour (step 1).

First, the discharge through each vertical column is evaluated. These discharges must represent the global water amount that seeps into each vertical water column, and will be used as a source term for each corresponding depth-integrated mesh in the calculation of the lateral diffusion.

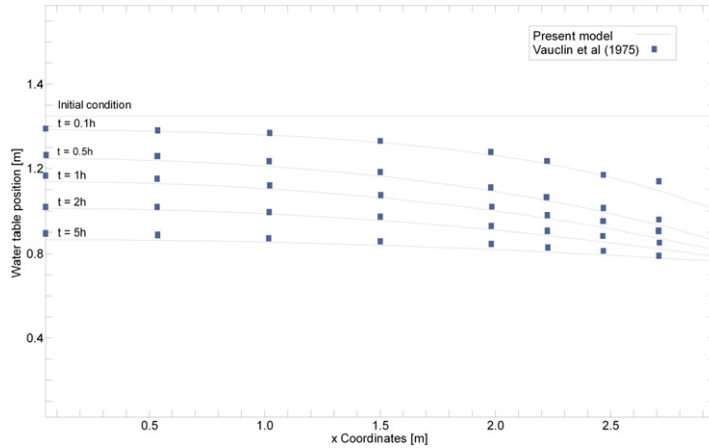


Fig. 5. The simulation of the water table position at different time of the experiment shows a good agreement with the experimental results.

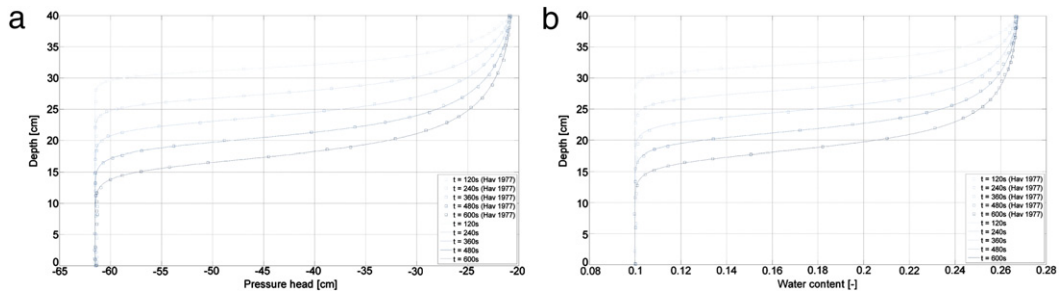


Fig. 6. The isovalues of—(left) water head (cm)—(right) water-content (—)—show agreement with the reference values.

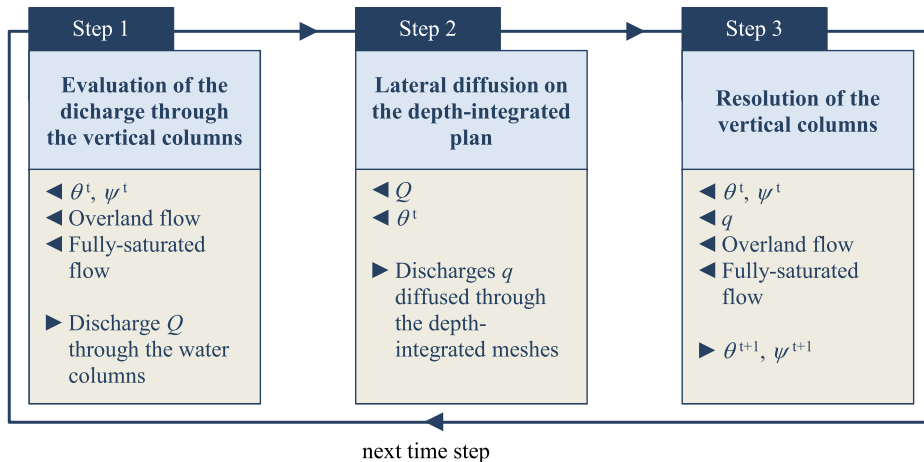


Fig. 7. Three specific sub-steps, which break down the water transfers into successive different physical process, are considered.

A mass balance on each vertical column enables to determine the mathematical formulation of these discharges. If we note  $\text{flux}_{\text{top}}$  as the water income from the overland flow and  $\text{flux}_{\text{bottom}}$  as the water income from the fully-saturated media, one has successively:

$$\text{flux}_{\text{top}} = \left\{ k_z |_{\text{top}} \left( \frac{\partial \psi}{\partial z} \Big|_{\text{top}} + 1 \right) \right. \quad (22)$$

$$\text{flux}_{\text{bottom}} = \left\{ k_z|_{\text{bottom}} \left( \frac{q_{\text{bottom}}}{\frac{\partial \psi}{\partial z}|_{\text{bottom}}} + 1 \right) \right. \quad (23)$$

with the first terms the specific discharge at the considered interface if the boundary condition is vonNeuman-type, and the second terms the flux resulting from the pressure head gradient at the interface if the boundary condition is Dirichlet-type, and evaluated as a function of the flow state at time step  $t$ , as specified on Fig. 7.

The evaluation of the transient discharge is directly obtained by the balance between these two fluxes.

The second step consists of the calculation of the diffused lateral flow on the depth-integrated plan. As the water incomes are known by step 1 (Fig. 8), the domain can be considered impervious, and Eq. (21) is applied to proceed to the calculation. The initial condition is the depth average of the water content at time step  $t$ .

Once the solution is obtained on the whole domain, it is possible to evaluate the fluxes on the edges between the meshes, that is the quantitative way the water has diffused. To do this, the Darcy equation ((1)(b)) is used, with the specificity that the discharges  $q$  are evaluated along the horizontal axis for each edge (Fig. 9).

Finally, the calculation of the vertical 1D column is performed using Eq. (20) for each column, and the solution is obtained on the whole domain.

The initial conditions, as specified on Fig. 7, are the water content and the pressure head at time step  $t$ . The boundary conditions consist in a weighting of the boundary conditions coming from the coupling with the bounded domains and the lateral discharges  $q$  evaluated at the second sub-step (Fig. 10).

The global scheme of integration is mass conservative. For the first step, the coupling with the external flows is such that the mass compatibility is ensured, that is, an iterative process is launched in order to assess the appropriateness of mass input and storage capacity. For the second step and the third step, the numerical scheme (18) is well-known as conservative [23]. Finally, from one step to another, the different discharges are unchanged, and thus there could be no losses. Furthermore, the mass balance is evaluated at each time step and one can assess its truthfulness, the input fluxes are compared with the storage during the time step  $\Delta t$ , and the relative error is measured.

## 6. Results and observations

The model needs to be assessed in terms of results strictly speaking, in order to validate the assertion made that the proposed method allow a reliable representation of the physical behaviour in the framework stated in the introductory sections.

Moreover, the computational properties of the proposed method have to be appraised. The time of execution must be discussed with regard to the full two-dimensional resolution on one hand, but also to the more simplistic one-dimensional infiltration law on the other hand. Thus, not only the save in time is analysed but also the extra cost with respect to common ways of dealing with this problem.

As for now, the implementation of our model restricts the possible tests to two-dimensional cross-sectional test cases for the same reasons as pointed in the introduction of Section 4.

### 6.1. Assessment of the proposed method in terms of physical behaviour

In order to allow a pertinent discussion as for the validity of the proposed method, some performance tests have been imagined.

From simplistic uniform and punctual infiltration test cases to more refined time and space distributed phenomena, two-dimensional comparisons between the proposed model and the full two-dimensional model are being made about the fluxes distribution and more especially about the mean level of water content in the unsaturated soil at different times of the process.

In this paper, 4 of these are presented:

- uniform and constant infiltration;
- isolated-punctual and constant infiltration;
- multi-punctual and constant infiltration;
- multi-punctual and variable infiltration.

For all of these, a sandy clay loam soil of 400 (cm) depth is considered, modelled by a Brooks–Corey water-retention curve [44]; with  $\theta_s = 0.398$  (–),  $\theta_r = 0.398$  (–),  $\varphi_b = -59.41$  (cm),  $\lambda = 0.318$  (–),  $K_s = 0.43$  (cm/h). The initial condition is a constant water content ( $q = 0.235$ ), all the boundaries are considered impermeable except at the top and the infiltration rate is the saturated hydraulic conductivity. For all the graphs depicted below, the lines represent the two-dimensional model, while the markers represent the original proposed model.

The first test case consists of a validation, since there are theoretically no transferred discharges between vertical columns (Fig. 11).

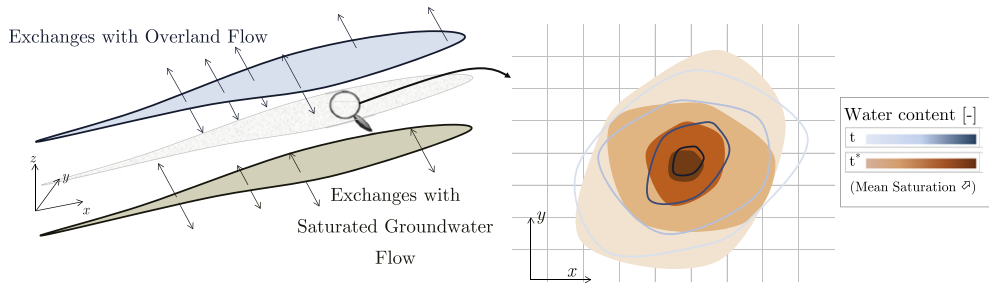


**Fig. 8.** With the first two steps, the lateral diffusion of the water incomes due to the overland flow at the top and the fully-saturated groundwater flow at the bottom is performed, giving a solution in terms of depth-integrated pressure head and water content on the whole domain.

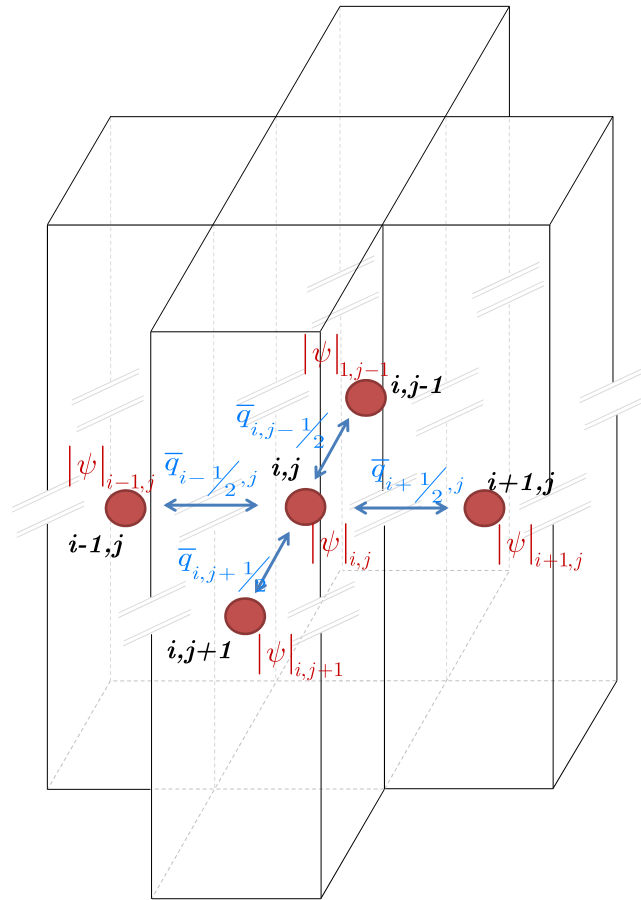


**Fig. 9.** The lateral discharges between depth-integrated cells are calculated.

The second test case depicts the opposite extreme of an isolated punctual infiltration. The interest of this theoretical test case – it should never be modelled because it is physically meaningless – is to assess the behaviour of horizontal transfer (Fig. 12).

The third test case, by multiplying the number of punctual infiltrations, depicts a more realistic phenomenon. It consists of 3 sources shared uniformly on the surface, and enables us to judge the pertinence of the proposed method on more physical process (Fig. 13).

The last test case is similar to the third one except for the fact that the infiltration rate is a series of sudden variations from the saturated hydraulic conductivity to zero during 6 h:

- a. 0 h → 2 h,  $q_{in} = K_S$ ;
- b. 2 h → 4 h,  $q_{in} = 0$ ;
- c. 4 h → 6 h,  $q_{in} = K_S$ .



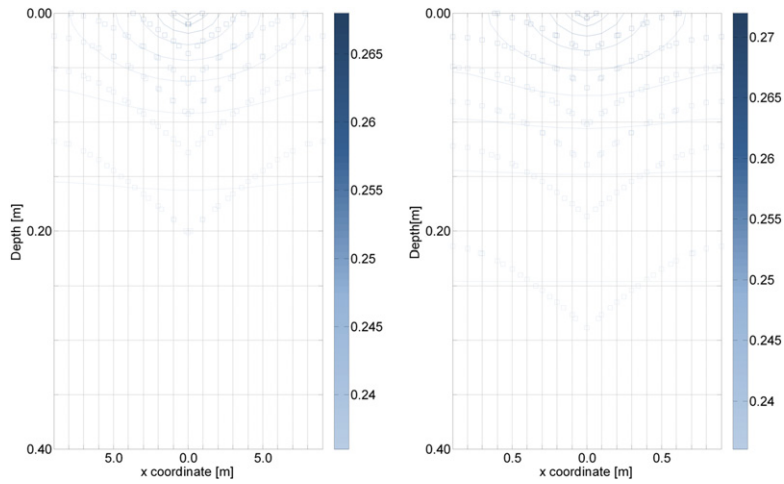


**Fig. 12.** The isolated-punctual and constant infiltration test case (ii) enables to observe that the ratio of transferred water with respect to infiltrated water is of a good order.

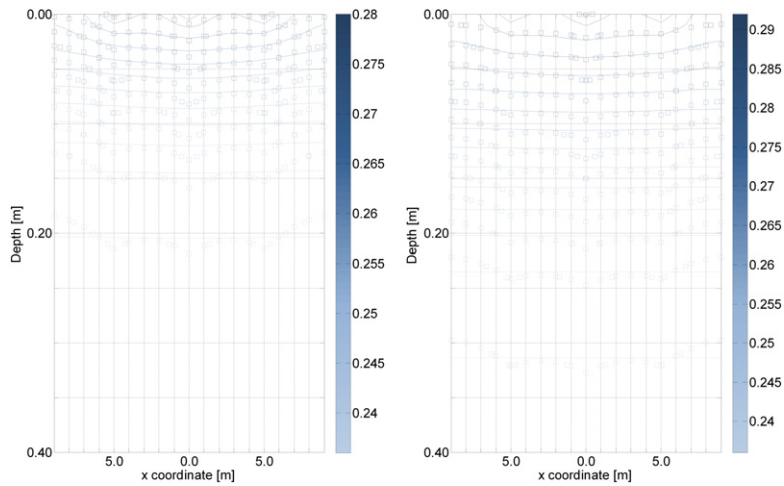


**Fig. 13.** The multi-source and constant infiltration test case (iii) enables to affirm that the more the sources are shared, the more accurate the solution is.

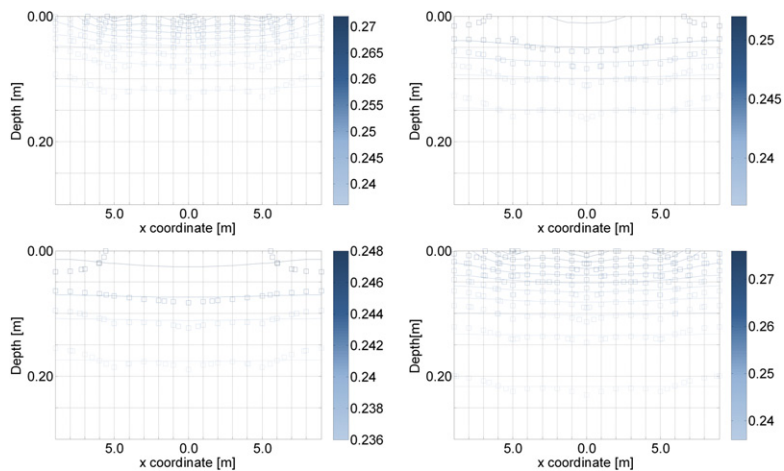


**Fig. 14.** A variable infiltration (iv) is depicted with a good agreement even in case of de-saturation when the infiltration stops.

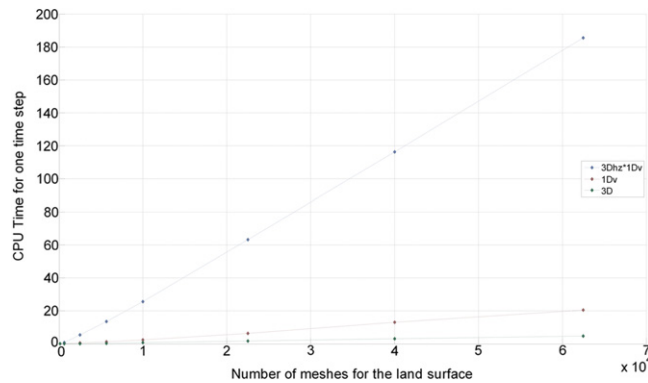


Fig. 15. The gain in time is enormous, and it increases with the dimensions of the surface.

## 7. Conclusions

In this paper, an original model is introduced, that enables to solve the groundwater flow in the unsaturated zone accurately with low computational resources required (see Fig. 15).

The idea of decoupling the vertical and horizontal transfers allows a fast resolution, by reducing significantly the number of unknowns in an individual linear system. Moreover, the vertical process is thus depicted by a one-dimensional equation, which makes a direct resolution of the linear system possible.

The proposed model reveals effective for severe infiltration zone types, even in case of variable income. In fact, the water flow is well represented in all directions, with propagation times that are rather reliable.

The model can therefore be used in an objective to evaluate the water exchanges with both the surface and the aquifers, to estimate the water content and the pressure on the whole subsoil, and to represent the lateral diffusion, enabling this way the calculation of more complex process than simply flood hydrographs. Eventually, it can be used as a tool for hydrological modelling in the context of climate changes, with simulation over large period of time possible thanks to these features.

Finally, the proposed method enables a gain in computation time that logically increases with the number of overland surface meshes. Besides, even for large catchment areas, the loss in time compared to single one-dimensional models remains limited, even more in view of the advantages brought up.

The main drawback of the method is its inability to deal with heterogeneous soil. However, further researches have already been conducted in order to permit in a certain way the consideration of a more realistic soil composition. Besides, other works are currently achieved about the coupling with the saturated zone and the runoff surface.

## References

- [1] P. Archambeau, Contribution à la modélisation de la genèse et de la propagation des crues et inondations, in: ArGenCo, University of Liège, Liège, 2006.
- [2] S. Erpicum, P. Archambeau, S. Detrembleur, B.J. Dewals, M. Pirotton, Optimisation of hydroelectric power stations operations with WOLF package, in: 5th International Conference on Hydropower, Stavanger, 2005.
- [3] F. Kerger, P. Archambeau, S. Erpicum, B.J. Dewals, M. Pirotton, A fast universal solver for 1D continuous and discontinuous steady flows in rivers and pipes, *International Journal for Numerical Methods in Fluids* 66 (2011) 38–48.
- [4] F. Kerger, Modelling transient air–water flows in civil and environmental engineering, in: ArGenCo, University of Liège, Liège, 2011.
- [5] B.J. Dewals, P. Archambeau, S. Erpicum, T. Mouzelard, M. Pirotton, Coupled computations of highly erosive flows with WOLF software, in: K. Peter Holz Mutsuto Kawahara SWSY (Ed.), Proc. 5th Int. Conf. on Hydro-Science & -Engineering, Warsaw, 2002, p. 10.
- [6] B.J. Dewals, F. Rulot, S. Erpicum, P. Archambeau, M. Pirotton, Advanced topics in sediment transport modelling: non-alluvial beds and hyperconcentrated flows, in: INTECH (Ed.), Sediment Transport, 2011.
- [7] S. Erpicum, Y. Mao, M. Pirotton, A. Lejeune, Process-oriented pollutant transport modelling in rivers networks—application in the Xizhijiang River in China, in: 3rd Int. Symp. on Integrated Water Resources Management, Ruhr University, Bochum, Germany, 2006.
- [8] S. Erpicum, Optimisation objective de paramètres en écoulements à surface libre sur maillage multibloc, University of Liege, 2006, p. 364.
- [9] J. Ernst, B.J. Dewals, S. Detrembleur, P. Archambeau, S. Erpicum, M. Pirotton, Integrated flood risk analysis for assessing flood protection strategies, in: T. Gasmelseid (Ed.), Handbook of Research on Hydroinformatics: Technologies Theories and Applications, Igi Global, Hershey, 2010.
- [10] B.J. Dewals, S. Detrembleur, P. Archambeau, S. Erpicum, M. Pirotton, J. Ernst, Caractérisation micro-échelle du risque d'inondation: modélisation hydraulique détaillée et quantification des impacts socio-économiques, *Houille Blanche—Review International* 2 (2011) 28–34.
- [11] P. Archambeau, S. Erpicum, T. Mouzelard, M. Pirotton, Impact studies and water management with WOLFHEDRO: a new physically based hydrological solver, in: Proc. Int. Symposium on Environmental Hydraulics, Arizona State University, USA, 2001.
- [12] B. Khuat Duy, Modélisation spatialement distribuée et physiquement basée d'écoulements hydrologiques et hydrodynamiques pour l'aide à la gestion d'ouvrages hydrauliques, in: ArGenCo, University of Liège, Liège, 2011.
- [13] M.F. Pikul, R.L. Street, I. Remson, A numerical model based on coupled one-dimensional Richards and Boussinesq equations, *Water Resources Research* 10 (1974) 295–302.
- [14] A. Yakirevich, V. Borisov, S. Sorek, A quasi three-dimensional model for flow and transport in unsaturated and saturated zones: 1. Implementation of the quasi two-dimensional case, *Advances in Water Resources* 21 (1998) 679–689.
- [15] M. Kuznetsov, A. Yakirevich, Y.A. Pachepsky, S. Sorek, N. Weisbrod, Quasi 3D modeling of water flow in vadose zone and groundwater, *Journal of Hydrology* 450–451 (2012) 140–149.
- [16] N.K.C. Twarakavi, J. Šimůnek, S. Seo, Evaluating interactions between groundwater and vadose zone using the hydrus-based flow package for modflow, *Vadose Zone Journal* 7 (2008) 757–768.

- [17] G. Vachaud, M. Vauclin, Comments on 'A numerical model based on coupled one-dimensional Richards and Boussinesq equations' by Mary F. Pikul, Robert L. Street, and Irwin Remson, *Water Resources Research* 11 (1975) 506–509.
- [18] S. Brouyère, Etude et modélisation du transport et du piégeage des solutés en milieu souterrain variablement saturé, in: FSA—Département ArGenCo, Université de Liège, Liège, 2001, p. 640.
- [19] Y. Shao, P. Irannejad, On the choice of soil hydraulic models in land-surface schemes, *Boundary-Layer Meteorology* 90 (1999) 83–115.
- [20] M. Vauclin, G. Vachaud, J. Khanji, Two dimensional numerical analysis of transient water transfer in saturated–unsaturated soils, in: G.C. Vansteenkiste (Ed.), *Modeling and Simulation of Water Resources Systems*, Ghent, Belgium, 1975.
- [21] M. Vauclin, D. Khanji, G. Vachaud, Experimental and numerical study of a transient, two-dimensional unsaturated–saturated water table recharge problem, *Water Resources Research* 15 (1979) 1089–1101.
- [22] R. Haverkamp, M. Vauclin, J. Touma, P.J. Wierenga, G. Vachaud, A comparison of numerical simulation models for one-dimensional infiltration, *Soil Science Society of America Journal* 41 (1977) 285–294.
- [23] M.A. Celia, E.T. Bouloutas, R.L. Zarba, A general mass-conservative numerical solution for the unsaturated flow equation, *Water Resources Research* 26 (1990) 1483–1496.
- [24] C. Paniconi, M. Putti, A comparison of Picard and Newton iteration in the numerical solution of multidimensional variably saturated flow problems, *Water Resources Research* 30 (1994) 3357–3374.
- [25] Y. Saad, M.H. Schultz, GMRES: a generalized minimal residual algorithm for solving nonsymmetric linear systems, *SIAM Journal on Scientific and Statistical Computing* 7 (1986) 856–869.
- [26] K. Huang, B.P. Mohanty, M.T. van Genuchten, A new convergence criterion for the modified Picard iteration method to solve the variably saturated flow equation, *Journal of Hydrology* 178 (1996) 69–91.
- [27] S.P. Neuman, Saturated–unsaturated seepage by finite elements, *Journal of the Hydraulics Division* 99 (1973) 2235–2250.
- [28] S.P. Neuman, Comment on “Some new procedures for numerical solution of variably saturated flow problems” by Richard L. Cooley, *Water Resources Research* 21 (1985) 886.
- [29] J.C. van Dam, R.A. Feddes, Numerical simulation of infiltration, evaporation and shallow groundwater levels with the Richards equation, *Journal of Hydrology* 233 (2000) 72–85.
- [30] I. Borsi, A. Farina, M. Primicerio, A rain water infiltration model with unilateral boundary condition: qualitative analysis and numerical simulations, *Mathematical Methods in the Applied Sciences* 29 (2006) 2047–2077.
- [31] B. Khuat Duy, P. Archambeau, S. Erpicum, B.J. Dewals, M. Piroton, Assessment of flood mitigation solutions using a hydrological model and refined 2D hydrodynamic simulations, in: *European Geosciences Union General Assembly 2009*, European Geosciences Union, Vienna, Austria, 2009.
- [32] R. Paulus, P. Archambeau, S. Erpicum, B.J. Dewals, M. Piroton, On the assessment of a modified diffusion-wave approximation model in the framework of overland flow, in: E.M. Valentine (Ed.), *34th IAHR World Congress—Balance and Uncertainty in a Changing World*, Brisbane, Australia, 2011.
- [33] S.D. Conte, C.W. de Boor, *Elementary Numerical Analysis: An Algorithmic Approach*, McGraw-Hill Higher Education, 1980.
- [34] G. Manzini, S. Ferraris, Mass-conservative finite volume methods on 2-D unstructured grids for the Richards equation, *Advances in Water Resources* 27 (2004) 1199–1215.
- [35] R.G. Baca, J.N. Chung, D.J. Mulla, Mixed transform finite element method for solving the non-linear equation for flow in variably saturated porous media, *International Journal for Numerical Methods in Fluids* 24 (1997) 441–455.
- [36] A.W. Warrick, Numerical approximations of Darcian flow through unsaturated soil, *Water Resources Research* 27 (1991) 1215–1222.
- [37] M. Vauclin, G. Vachaud, J. Khanji, Two dimensional numerical analysis of transient water transfer in saturated–unsaturated soils, in: G.C. Vansteenkiste (Ed.), *Computer Simulation of Water Resources Systems*, Ghent, Belgium, 1975, pp. 299–323.
- [38] T.P. Clement, W.R. Wise, F.J. Molz, A physically based, two-dimensional, finite-difference algorithm for modeling variably saturated flow, *Journal of Hydrology* 161 (1994) 71–90.
- [39] T.B. Thoms, R.L. Johnson, R.W. Healy, User's guide to the variably saturated flow (VSF) process for modflow, in: *U.S.G.S.T.a.M. 6-A18* (Ed.), 2006, p. 58.
- [40] W.H. Gardner, J.C. Hsieh, *Water movement in soils*, USA, 1959.
- [41] R. Paulus, P. Archambeau, S. Erpicum, B.J. Dewals, M. Piroton, Handling of the 3D behaviour of the unsaturated layer using a vertical 1D model for the Richards equation along with diffusive horizontal fluxes, in: E.M. Valentine (Ed.), *34th IAHR World Congress—Balance and Uncertainty in a Changing World*, Brisbane, Australia, 2011.
- [42] M.T. van Genuchten, D.R. Nielsen, On describing and predicting the hydraulic properties of unsaturated soils, *Annales Geophysicae* 3 (1985) 615–627.
- [43] M.T. van Genuchten, A closed-form equation for predicting the hydraulic conductivity of unsaturated soils, *Soil Science Society of America Journal* 44 (1980) 892–898.
- [44] J.W. Rawls, D.L. Brakensiek, K.E. Saxton, Estimation of soil water properties, *Transactions of the ASAE* 25 (1982) 1316–1320.